

Coupled nitrogen and oxygen isotope measurements of nitrate along the eastern North Pacific margin

Daniel M. Sigman,¹ Julie Granger,² Peter J. DiFiore,¹ Moritz M. Lehmann,³ Ruby Ho,¹ Greg Cane,¹ and Alexander van Geen⁴

Received 12 January 2005; revised 21 June 2005; accepted 31 August 2005; published 23 December 2005.

[1] Water column depth profiles along the North Pacific margin from Point Conception to the tip of Baja California indicate elevation of nitrate (NO_3^-) $^{15}\text{N}/^{14}\text{N}$ and $^{18}\text{O}/^{16}\text{O}$ associated with denitrification in the oxygen-deficient thermocline waters of the eastern tropical North Pacific. The increase in $\delta^{18}\text{O}$ is up to 3‰ greater than in $\delta^{15}\text{N}$, whereas our experiments with denitrifier cultures in seawater medium indicate a 1:1 increase in NO_3^- $\delta^{18}\text{O}$ and $\delta^{15}\text{N}$ during NO_3^- consumption. Moreover, the maximum in NO_3^- $\delta^{18}\text{O}$ is somewhat shallower than the maximum in NO_3^- $\delta^{15}\text{N}$. These two observations can be summarized as an “anomaly” from the 1:1 $\delta^{18}\text{O}$ -to- $\delta^{15}\text{N}$ relationship expected from culture results. Comparison among stations and with other data indicates that this anomaly is generated locally. The anomaly has two plausible interpretations: (1) the addition of low- $\delta^{15}\text{N}$ NO_3^- to the shallow thermocline by the remineralization of newly fixed nitrogen, or (2) active cycling between NO_3^- and NO_2^- (coupled NO_3^- reduction and NO_2^- oxidation) in the suboxic zone.

Citation: Sigman, D. M., J. Granger, P. J. DiFiore, M. M. Lehmann, R. Ho, G. Cane, and A. van Geen (2005), Coupled nitrogen and oxygen isotope measurements of nitrate along the eastern North Pacific margin, *Global Biogeochem. Cycles*, 19, GB4022, doi:10.1029/2005GB002458.

1. Introduction

[2] The oceanic budget of biologically available (or “fixed”) nitrogen is poorly understood. Estimates of the global rate of nitrogen (N) loss by denitrification would leave the ocean N budget far out of balance unless N_2 fixation rates are much higher than previously estimated [Brandes and Devol, 2002; Codispoti et al., 2001; Middelburg et al., 1996]. While such imbalances cannot be ruled out, the stability of atmospheric CO_2 and of the N isotopic composition of deep sea sediments over the last ~5 kyr argues against such extreme imbalances [Deutsch et al., 2004; Kienast, 2000].

[3] Direct measurements of N fluxes in the ocean (e.g., N_2 fixation, denitrification, NO_3^- assimilation, and nitrification) cannot, by themselves, provide a reliable picture of the ocean N cycle. Temporal and spatial complexity, combined with the limitations of shipboard sampling of the ocean, lead to uncertainty in the extrapolation of these measurements to regional and global fluxes. Moreover, assays for N

transformations can perturb the samples they are attempting to measure. For these reasons, biogeochemical parameters in ocean water have become important as more integrative measures of the rates of N fluxes.

[4] Deviations in the $[\text{NO}_3^-]$ -to- $[\text{PO}_4^{3-}]$ relationship from the “Redfield” relationship driven by algal assimilation and remineralization are used to study the rates and distributions of both N_2 fixation and denitrification. “N*”, defined as $[\text{NO}_3^-] - 16 \times [\text{PO}_4^{3-}] + 2.9$ (in $\mu\text{mol}/\text{kg}$) [Deutsch et al., 2001], quantifies excesses and deficits in NO_3^- relative to the globally derived $[\text{NO}_3^-]$ -to- $[\text{PO}_4^{3-}]$ relationship, indicating regions of N_2 fixation and denitrification, respectively. When combined with some measure of ocean circulation, rates of these processes can be derived [Deutsch et al., 2001; Gruber and Sarmiento, 1997]. While this use of nutrient data is extremely powerful, it has limitations. First, deviations from the Redfield $[\text{NO}_3^-]$ -to- $[\text{PO}_4^{3-}]$ relationship may not always be due to N inputs or outputs, arising instead from variations in the stoichiometry of nutrient uptake and remineralization. Second and most relevant here, NO_3^- inputs and losses partially erase one another if they occur in the same water or if their host waters are mixed in a way that cannot be reconstructed.

[5] The complementary measurement of NO_3^- $^{15}\text{N}/^{14}\text{N}$ can address the first limitation described above. The N isotopes provide an additional test as to whether positive or negative N* in a given region is indeed driven by N_2 fixation or denitrification. Most of the deep ocean (>2 km) is homogenous in NO_3^- $\delta^{15}\text{N}$, at ~5‰ relative to atmospheric N_2 [Liu and Kaplan, 1989; Sigman et al., 2000]

¹Department of Geosciences, Princeton University, Princeton, New Jersey, USA.

²Department of Earth and Ocean Sciences, University of British Columbia, Vancouver, British Columbia, Canada.

³Geochemistry and Geodynamics Research Center (GEOTOP-UQAM-McGill), University of Quebec at Montreal, Montreal, Quebec, Canada.

⁴Lamont-Doherty Earth Observatory of Columbia University, Palisades, New York, USA.

($\delta^{15}\text{N}_{\text{sample}} = ((^{15}\text{N}/^{14}\text{N})_{\text{sample}}/(^{15}\text{N}/^{14}\text{N})_{\text{reference}} - 1) \times 1000\text{‰}$, where the $^{15}\text{N}/^{14}\text{N}$ reference is N_2 in air). N_2 fixation in the ocean introduces new fixed N with a $\delta^{15}\text{N}$ of ~ -2 – 0‰ relative to atmospheric N_2 [Carpenter et al., 1997; Delwiche et al., 1979; Hoering and Ford, 1960]. Thus inputs of newly fixed N can drive a regional decrease in the NO_3^- $\delta^{15}\text{N}$ of the shallow subsurface [Brandes et al., 1998; Karl et al., 2002; Knapp et al., 2005; Liu et al., 1996; Pantoja et al., 2002]. Denitrification preferentially consumes $^{14}\text{NO}_3^-$, so its occurrence leads to a marked increase in NO_3^- $\delta^{15}\text{N}$ in oceanic regions of suboxia [Altabet et al., 1999; Brandes et al., 1998; Cline and Kaplan, 1975; Liu and Kaplan, 1989; Voss et al., 2001].

[6] Moreover, the $^{15}\text{N}/^{14}\text{N}$ of NO_3^- can provide important constraints on the mechanisms of N inputs or losses. In particular, it can provide information on the importance of the sediments versus the water column as environments for denitrification [Brandes and Devol, 1997]. Denitrification in the ocean water column has yielded estimates of 20–30‰ for the isotope effect for denitrification [Altabet et al., 1999; Brandes et al., 1998; Cline and Kaplan, 1975; Liu and Kaplan, 1989; Sigman et al., 2003b; Voss et al., 2001], which is similar to at least some estimates from cultures [Barford et al., 1999; Mariotti et al., 1981] (the N isotope effect, $^{15}\epsilon$, is defined here as $(^{15}\text{k}/^{14}\text{k} - 1) \times 1000\text{‰}$, where ^{14}k and ^{15}k are the rate coefficients of the reactions for the ^{14}N - and ^{15}N -bearing forms of NO_3^- , respectively). By contrast, sedimentary denitrification in a variety of environments causes very little net isotope enrichment of oceanic NO_3^- [Brandes and Devol, 1997, 2002; Lehmann et al., 2004; Sebilo et al., 2003; Sigman et al., 2001]. This yields a critical constraint on the relative importance of water column versus sedimentary denitrification on a global scale [Brandes and Devol, 2002] and in isolated basins [Sigman et al., 2003b].

[7] However, the N isotopes do not escape the second weakness described above for the N-to-P approach: Because N_2 fixation and denitrification have counteracting effects on both N^* and NO_3^- $\delta^{15}\text{N}$, gross fluxes from either process cannot be determined with sufficient accuracy. For instance, N_2 fixation in the tropical and subtropical Pacific surface adds new NO_3^- to the Pacific thermocline, increasing N^* and decreasing NO_3^- $\delta^{15}\text{N}$, while denitrification removes low- $\delta^{15}\text{N}$ NO_3^- from suboxic regions of the eastern Pacific, lowering N^* and raising the $\delta^{15}\text{N}$ of the residual NO_3^- . If the two processes occur in the same region or if waters from these regions mix vigorously, the tracer signals of both processes are reduced [Deutsch et al., 2001].

[8] Previous coupled studies of NO_3^- N and O isotopes have observed a strong correlation between these two isotope systems, with both NO_3^- $\delta^{15}\text{N}$ and $\delta^{18}\text{O}$ increasing as NO_3^- is consumed by denitrification. Freshwater studies observe an O:N ratio for isotope effects ($^{18}\epsilon$: $^{15}\epsilon$) of ~ 0.5 – 0.6 , for their respective isotope systems [Botcher et al., 1990; Lehmann et al., 2003; Mengis et al., 1999]. However, our culture experiments with denitrifiers in seawater yield an $^{18}\epsilon$: $^{15}\epsilon$ of ~ 1 [Granger et al., 2004a], as does a field study of an enclosed marine basin [Sigman et al., 2003b]. This fits with our previous observations for algal NO_3^- assimilation, for which we also observe an $^{18}\epsilon$: $^{15}\epsilon$ of ~ 1

over a broad range of amplitudes for the isotope effect [Casciotti et al., 2002; Granger et al., 2004b]. That we observe the same $^{18}\epsilon$: $^{15}\epsilon$ for both denitrification and NO_3^- assimilation is consistent with evidence that NO_3^- reduction is the dominant cause of fractionation in both processes [Needoba et al., 2004; Shearer et al., 1991]. Thus, while we have much to learn about the N:O fractionation ratios, NO_3^- assimilation and denitrification, the processes of NO_3^- consumption with the greatest effects on oceanic NO_3^- distributions, apparently cause similar isotope fractionation of N and O in NO_3^- .

[9] Unlike the consumption of NO_3^- , NO_3^- production appears to have very different effects on the N and O isotopes of NO_3^- . In the open ocean subsurface, at least in oxic waters, almost all of the ammonium generated from organic N is eventually oxidized to NO_3^- , so that the N isotope effects associated with ammonium production and nitrification do not impact the $\delta^{15}\text{N}$ of NO_3^- produced. In this case, the $\delta^{15}\text{N}$ of newly produced NO_3^- is primarily controlled by the $\delta^{15}\text{N}$ of the organic matter being remineralized. The $\delta^{18}\text{O}$ of newly produced NO_3^- obviously does not depend on the isotopic composition of the organic matter being remineralized.

[10] Biochemical studies have derived mechanisms for ammonium oxidation to nitrite (NO_2^-) in which one O atom is donated from O_2 and the other from water [Andersson et al., 1982]. NO_2^- oxidation to NO_3^- involves the donation of O only from water [Dispirito and Hooper, 1986; Kumar et al., 1983]. On this basis, the traditional interpretation has been that two thirds of the O atoms in NO_3^- should originate from water and one third should originate from O_2 [Böhlke et al., 1997; Durka et al., 1994; Kendall, 1998; Wassenaar, 1995]. However, the same biochemical studies also demonstrated a strong nitrifier-catalyzed nitrite-water exchange of O atoms [Andersson et al., 1982]. On the basis of these observations, it is likely that much less than one out of two O atoms in NO_2^- comes from O_2 [Casciotti et al., 2002]. A culture experiment in which *Nitrosomonas europaea* produces NO_2^- in the presence of ^{18}O -labeled water indicates that at least 50% of the O atoms in NO_2^- have undergone exchange with water [Casciotti, 2002], such that at least 5 out of the 6 O atoms in NO_3^- originate from water (i.e., 1 or less out of the 6 comes from O_2). It is also possible that catalysis of exchange with water occurs during the oxidation of NO_2^- to NO_3^- [Dispirito and Hooper, 1986], reducing further the effective contribution of O atoms from O_2 and increasing the contribution from H_2O .

[11] Measurements to date from the ocean indicate that away from regions of known denitrification, subsurface NO_3^- $\delta^{18}\text{O}$ varies relatively little and is close to the ambient water ($0 \pm 1\text{‰}$ or $3 \pm 1\text{‰}$ different from it; see auxiliary material, endnote i in Auxmat1.txt¹) the ambient water ($\delta^{18}\text{O}_{\text{sample}} = ((^{18}\text{O}/^{16}\text{O})_{\text{sample}}/(^{18}\text{O}/^{16}\text{O})_{\text{reference}} - 1) \times 1000\text{‰}$, where the reference is Vienna Standard Mean Ocean Water (VSMOW); see section 2). Deep NO_3^- $\delta^{18}\text{O}$ is within $\pm 1\text{‰}$ among regions with very different deep O_2

¹Auxiliary material is available at <ftp://ftp.agu.org/apend/gb/2005GB002458>.

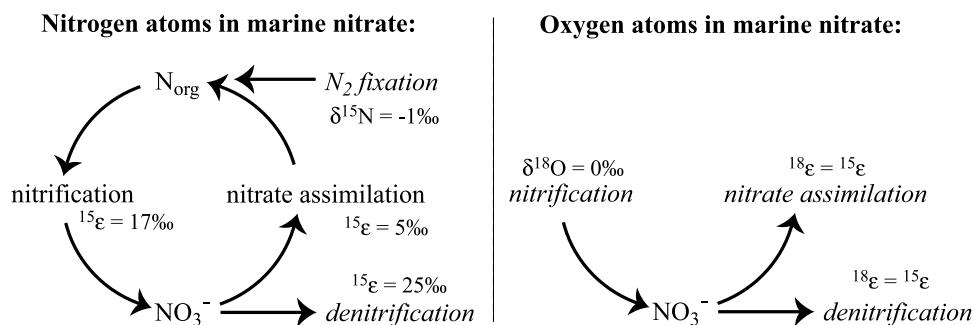


Figure 1. The major N transformations in the ocean as seen from the perspective of the (a) N atoms and (b) O atoms of nitrate (NO_3^-). Italicized fluxes indicated absolute sources or sinks of NO_3^- -N or NO_3^- -O. Characteristic estimates for N isotope effects ($^{15}\epsilon$) and $\delta^{15}\text{N}$ (relative to air N_2) are given in Figure 1a [Sigman and Casciotti, 2001; Casciotti et al., 2003]. The estimates for O isotope effects ($^{18}\epsilon$) and $\delta^{18}\text{O}$ (relative to VSMOW) are based on the available marine field measurements and laboratory culture studies of algae and denitrifiers in seawater media [Casciotti et al., 2002; Granger et al., 2004a, 2004b].

concentration (the Bering Sea, the North Pacific, the Southern Ocean, and the North Atlantic), arguing against a strong influence from O_2 $\delta^{18}\text{O}$ [Casciotti et al., 2002; Lehmann et al., 2005] (A. Knapp, unpublished data, 2005). This is consistent with ambient water being the dominant source of the O atoms in NO_3^- , although much work remains to be done on this question.

[12] In general, the additional insight that NO_3^- $\delta^{18}\text{O}$ brings to measurements of NO_3^- $\delta^{15}\text{N}$ and N^* involves the processes that are not captured by the O isotopes (Figure 1). As seen from the N atom in NO_3^- , NO_3^- assimilation and nitrification are part of an internal cycle within the ocean that should cause no net change in the mean $\delta^{15}\text{N}$ of ocean NO_3^- over time. N_2 fixation and denitrification (plus additional smaller terms) comprise the input/output budget of fixed N and control the mean $\delta^{15}\text{N}$ of ocean NO_3^- [Brandes and Devol, 2002; Deutsch et al., 2004]. In contrast, for the O atoms in NO_3^- , nitrification is an absolute input, while both NO_3^- assimilation and denitrification are absolute sinks. The $\delta^{18}\text{O}$ of newly produced NO_3^- does not depend on the origin of NH_4^+ being nitrified, be it from newly fixed N, from the biomass of phytoplankton growing in a NO_3^- -rich environment, or from biomass of phytoplankton in a NO_3^- -poor environment that assimilate all of the NO_3^- supplied to them.

[13] This fundamental difference between the N and O isotopes of NO_3^- allows their coupled measurement to separate processes that overprint one another when they are monitored using NO_3^- $\delta^{15}\text{N}$ alone. For instance, with the added constraint of NO_3^- $\delta^{18}\text{O}$, it should be possible to separate and quantify the impacts of N_2 fixation and denitrification. The N and O isotopes of NO_3^- are fractionated to the same extent by denitrification. Thus NO_3^- becomes enriched in both ^{15}N and ^{18}O as denitrification proceeds. The difference between the two isotope systems arises with their different sensitivities to N_2 fixation. While the nitrification of newly fixed N will work to lower the $\delta^{15}\text{N}$ of subsurface NO_3^- , the $\delta^{18}\text{O}$ of NO_3^- produced by nitrification is insensitive to the origin of the N being remineralized in the subsurface. Thus O isotopes may indicate when the impact of N_2 fixation has caused

NO_3^- $\delta^{15}\text{N}$ (and N^*) to underestimate the NO_3^- lost to denitrification.

[14] At the same time, the O isotopes may record other gross fluxes of NO_3^- that do not impact the N isotopes. For instance, if NO_3^- is reduced to some other form (organic N, NH_4^+ , or NO_2^-) and then oxidized back to NO_3^- without any N loss, the $\delta^{15}\text{N}$ of NO_3^- is constrained by mass balance to remain unchanged, whereas the $\delta^{18}\text{O}$ of NO_3^- may change (Figure 1). The direction in which $\delta^{18}\text{O}$ changes will depend on whether the $\delta^{18}\text{O}$ of the NO_3^- removed is higher or lower than the $\delta^{18}\text{O}$ of the NO_3^- added back. If the NO_3^- added back is higher in $\delta^{18}\text{O}$ than that removed, then the NO_3^- $\delta^{18}\text{O}$ will drift upward. Because isotope discrimination during NO_3^- reduction often causes the $\delta^{18}\text{O}$ of the consumed NO_3^- to be less than $\delta^{18}\text{O}$ of newly produced NO_3^- , it will generally be the case that NO_3^- $\delta^{18}\text{O}$ will increase relative to $\delta^{15}\text{N}$ with the rate of an internal cycle of NO_3^- consumption and production.

[15] Here we use the coupled N and O isotopes of water column nitrate as complementary constraints on the N transformations at work in and nearby the eastern tropical North Pacific denitrification zone. Our central new observation is that the $\delta^{18}\text{O}$ of NO_3^- is up to 3‰ more elevated than is its $\delta^{15}\text{N}$ relative to “background” (e.g., deep open ocean) NO_3^- , with the greatest deviation between the two isotope systems at ~ 100 m shallower than the previously described $\delta^{15}\text{N}$ maximum. Given that our culture experiments indicate a 1:1 $\delta^{18}\text{O}:\delta^{15}\text{N}$ elevation by denitrification, we attempt to identify and quantify the process responsible for the deviation of the O and N isotopes from denitrification-only behavior.

2. Materials and Methods

2.1. Sample Collection

[16] Water samples were collected through the water column by hydrocast off the California coast from Point Conception to the southern tip of Baja California during coring cruise OXMZ01MV aboard the RV *Melville* in November of 1999 (Figure 2) [van Geen, 2001]. Samples

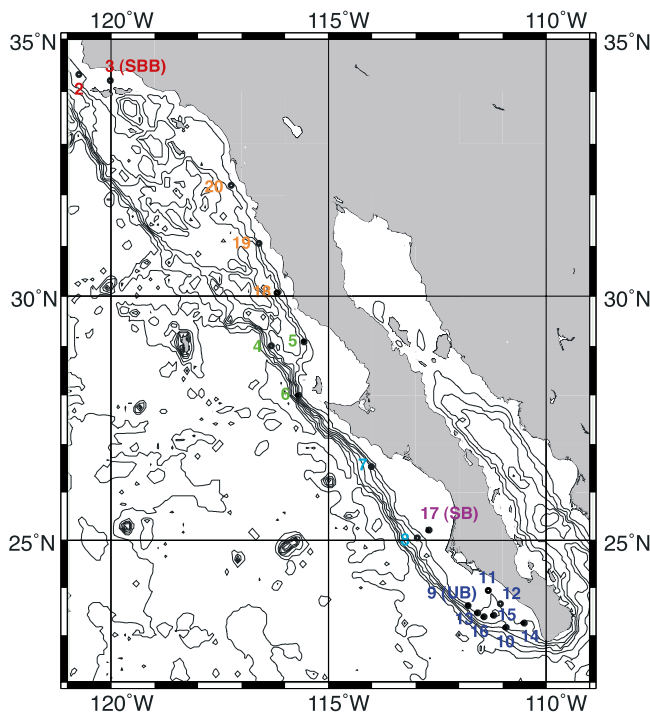


Figure 2. Station locations from coring cruise OXMZ01MV aboard the RV *Melville* in November of 1999. Stations 8 to 17 have mid-depth $[O_2]$ minima reaching below $3 \mu\text{M}$, while station 7 reaches a minimum $[O_2]$ of $\sim 5 \mu\text{M}$; the empirical upper limit for active water column denitrification is $\sim 4 \mu\text{M}$ [Lipschultz et al., 1990; Codispoti et al., 2001]. The color scheme is used in subsequent Figures 3, 4a, 4c, and 6. Station 3 samples waters in the Santa Barbara Basin (SBB), which has a sill depth of $\sim 475 \text{ m}$. Station 17 samples waters in the Soledad Basin (SB), which has a sill depth of $\sim 300 \text{ m}$. Station 9 samples waters of an unnamed basin (UB) with a sill depth of $\sim 460 \text{ m}$ [van Geen et al., 2003]. All stations were sampled near the depth of the seafloor. Contours are every 750 m .

were collected in acid- and distilled water-rinsed polyethylene bottles after two rinses with sample water and were preserved by acidification to a pH of 2–3 with 50% reagent-grade hydrochloric acid. Upon arrival at the laboratory 4 months after collection, an aliquot of each sample was frozen, and these aliquots were used for NO_3^- N and O isotope analysis.

2.2. Dissolved Oxygen and Nutrient Concentration Measurements

[17] During OXMZ01MV, the concentrations of phosphate (PO_4^{3-}), nitrate (NO_3^-), and nitrite (NO_2^-) were measured at sea by automated colorimetric methods, and the concentration of dissolved O_2 was measured by Winkler titration. In the hydrocast profiles from OXMZ01MV, $[\text{NO}_2^-]$ was less than $0.1 \mu\text{M}$ in all but one 50-m sample and was typically less than $0.05 \mu\text{M}$. This is much lower than measured at lower latitudes along the eastern tropical

Pacific margin [Codispoti et al., 1986; Lipschultz et al., 1990] but fits with previously reported distributions [Cline and Richards, 1972] (see endnote ii in Auxmat1.txt [Deutsch et al., 2001; Gruber and Sarmiento, 1997]).

2.3. NO_3^- Isotopic Analysis

[18] The $^{15}\text{N}/^{14}\text{N}$ and $^{18}\text{O}/^{16}\text{O}$ of NO_3^- were determined using the denitrifier method [Casciotti et al., 2002; Sigman et al., 2001]. Briefly, NO_3^- and NO_2^- are converted quantitatively to N_2O by a strain of bacterial denitrifier that lacks nitrous oxide reductase activity, and the product N_2O is extracted, purified, and analyzed by continuous flow isotope ratio mass spectrometry. Individual analyses are referenced to injections of N_2O from a pure gas cylinder and then standardized using international NO_3^- isotopic reference material IAEA-N3. The O isotope data are corrected for exchange with oxygen atoms from water during reduction of NO_3^- to N_2O [Casciotti et al., 2002], which is quantified by analysis of IAEA-N3 in ^{18}O -enriched water and was 5% or less for the analyses reported here. Reproducibility of replicates (which were analyzed for $\sim 75\%$ of the water samples) was generally consistent with previously reported analysis standard deviations of 0.2‰ for $\delta^{15}\text{N}$ and 0.5‰ for $\delta^{18}\text{O}$ (see endnote iii in Auxmat1.txt [Anbar and Gutmann, 1961; Böhlke et al., 2003; Bunton et al., 1952]).

[19] As stated above, referencing of $^{15}\text{N}/^{14}\text{N}$ to atmospheric N_2 and of $^{18}\text{O}/^{16}\text{O}$ to VSMOW was through comparison to the potassium nitrate (KNO_3) reference material IAEA-N3, with an assigned $\delta^{15}\text{N}$ of $+4.7\text{‰}$ [Gonfiantini et al., 1995] and reported $\delta^{18}\text{O}$ of $+22.7$ to $+25.6\text{‰}$ [Böhlke et al., 2003; Lehmann et al., 2003; Revesz et al., 1997; Silva et al., 2000]. We adopt here a $\delta^{18}\text{O}$ of 22.7‰ [Lehmann et al., 2003; Revesz et al., 1997; Silva et al., 2000], as we have used in previous publications. If we were to assume the most recent and highest estimate for the $\delta^{18}\text{O}$ of IAEA-N3 (25.6‰ , [Böhlke et al., 2003]), then the NO_3^- $\delta^{18}\text{O}$ of all of our samples would increase by $\sim 2.9\text{‰}$. Indeed, we expect that the new, higher $\delta^{18}\text{O}$ of IAEA-N3 will prove to be correct, but we wish to guard against using multiple different referencing schemes through time and thus will wait for corroboration of the results of Böhlke et al. [2003]. The O isotopic difference between NO_3^- reference IAEA-N3 (and indeed all NO_3^- references) and Vienna SMOW is not addressable with the denitrifier method, which can only measure isotopic differences among NO_3^- samples. The uncertainty in the isotopic difference between IAEA-N3 and VSMOW is an unfortunate source of uncertainty in our reported values. However, our focus here is on the variation of NO_3^- $^{18}\text{O}/^{16}\text{O}$ in the ocean, not its relationship to the isotope ratios found in seawater or other O-bearing materials. Our interpretation is not affected by a uniform shift in the $\delta^{18}\text{O}$ of all of our data sets relative to VSMOW, because all of the O isotope rules used in the calculations below are based on our own NO_3^- isotope data.

3. Results

[20] While N^* is generally negative throughout the eastern North Pacific (ENP), there is a thermocline-depth N^* minimum that indicates in situ denitrification or rapid

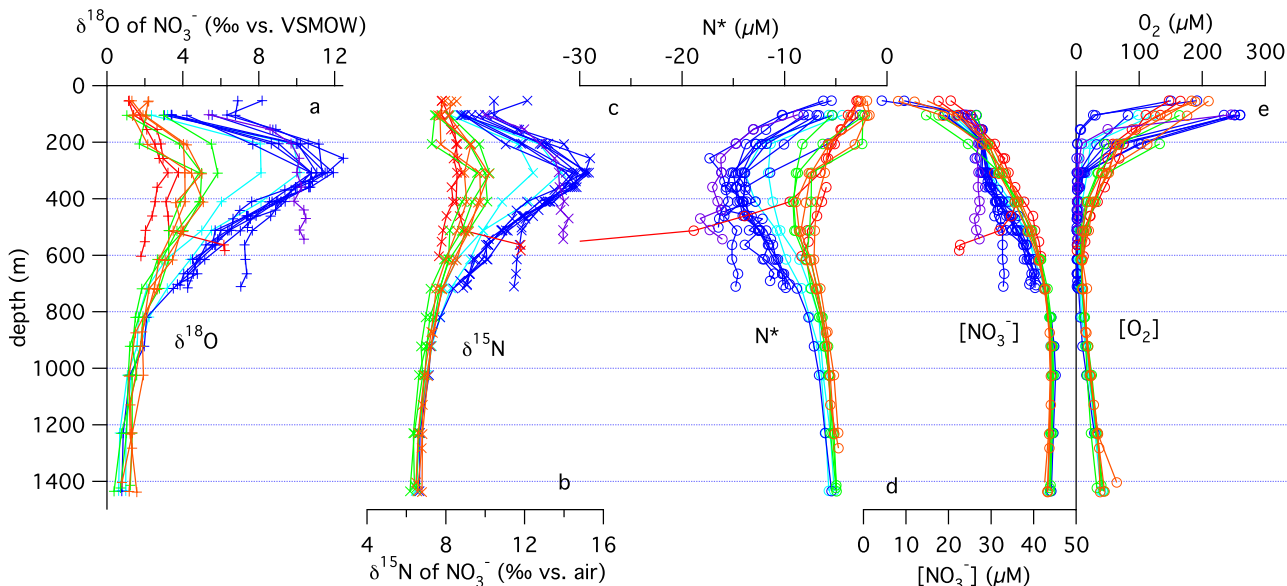


Figure 3. For all stations collected during OXMZ01MV, depth profiles of (a) $\text{NO}_3^- \delta^{18}\text{O}$, (b) $\text{NO}_3^- \delta^{15}\text{N}$, (c) N^* , (d) $[\text{NO}_3^-]$, and (e) $[\text{O}_2]$. Only analysis means are shown, as throughout the manuscript. Colors follow Figure 2. Stations 3 (Santa Barbara Basin, red), 17 (Soledad Basin, purple), and 9 (unnamed basin, deep blue) are apparent from their low N^* and high $\delta^{15}\text{N}$ and $\delta^{18}\text{O}$ at their bottoms. N^* in Santa Barbara Basin extends beyond the scale used here [Sigman *et al.*, 2003a].

exchange with a region of denitrification (Figure 3c). The N^* minimum is associated with the $[\text{O}_2]$ minimum (Figure 3e), with both O_2 depletion and the N^* minimum becoming more pronounced toward the south among our station locations. This is consistent with a requirement of very low $[\text{O}_2]$ ($<4 \mu\text{M}$ or so) for denitrification to proceed rapidly in the water column [Lipschultz *et al.*, 1990, and references therein]. The expectation based on the $[\text{O}_2]$ data is that water column denitrification is only active in the stations south of 25°N (blue symbols in Figure 3e). The N^* minimum and $\text{NO}_3^- \delta^{15}\text{N}$ and $\delta^{18}\text{O}$ maxima of the more northern stations result from the coastal undercurrent carrying northward these signals of denitrification [Altabet *et al.*, 1999; Liu and Kaplan, 1989; Sigman *et al.*, 2003b; Wooster and Jones, 1970].

[21] Comparison of profiles shows qualitatively that $\text{NO}_3^- \delta^{15}\text{N}/\delta^{14}\text{N}$ (Figure 3b) is strongly anti-correlated with N^* (Figure 3c), as would be expected from N isotope discrimination during denitrification. For a range of models of NO_3^- supply and consumption, a N isotope effect ($^{15}\epsilon$) for denitrification of $\sim 25\%$ has been estimated [Sigman *et al.*, 2003b], consistent with other studies referenced above. A much lower net isotope effect applies in the Santa Barbara Basin (station 3) because of denitrification in the sediments of that basin [Sigman *et al.*, 2003b].

[22] Within the sample set, the depth variations in the O and N isotopes of NO_3^- are strongly related (Figures 3a and 3b). A trend through the bulk of the data in a plot of $\text{NO}_3^- \delta^{18}\text{O}$ versus $\text{NO}_3^- \delta^{15}\text{N}$ has a slope of ~ 1.25 or higher (Figure 4). Our culture studies indicate that denitrifiers

in seawater express an O:N isotope effect ratio ($^{18}\epsilon:^{15}\epsilon$) of ~ 1 [Granger *et al.*, 2004a] (see endnote iv in Auxmat1.txt [Lehmann *et al.*, 2003]). In addition, NO_3^- assimilation by marine phytoplankton also exhibits an $^{18}\epsilon:^{15}\epsilon$ of ~ 1 [Casciotti *et al.*, 2002; Granger *et al.*, 2004b].

[23] The overall $\delta^{18}\text{O}:\delta^{15}\text{N}$ trend of 1.25 in the ENP data actually hides systematic depth-variations in the relationship between $\delta^{18}\text{O}$ and $\delta^{15}\text{N}$. At ~ 350 m, as N^* begins its upward increase and $\text{NO}_3^- \delta^{15}\text{N}$ begins to decrease, $\text{NO}_3^- \delta^{18}\text{O}$ holds steady or continues to increase an additional 100 m toward the surface before decreasing again, resulting in a $\text{NO}_3^- \delta^{18}\text{O}$ maximum that is ~ 100 m shallower than the $\delta^{15}\text{N}$ maximum and the N^* minimum. In our plots of $\text{NO}_3^- \delta^{18}\text{O}$ versus $\text{NO}_3^- \delta^{15}\text{N}$ (Figure 4), this leads to a “loop” (counterclockwise up) pattern: shoaling from the deepest samples, the isotopic composition of NO_3^- progresses upward and to the right along a slope of ~ 1.25 in $\delta^{18}\text{O}/\delta^{15}\text{N}$ space, then shifts toward a more vertical path as $\delta^{18}\text{O}$ continues to increase but $\delta^{15}\text{N}$ remains unchanged or decreases, then returns downward and to the left, typically reaching a $\delta^{18}\text{O}$ -to- $\delta^{15}\text{N}$ relationship at ~ 100 m that is similar to that of deep waters.

4. Interpretation

4.1. Quantifying the Deviation Between NO_3^- O and N Isotopes in the Thermocline

[24] We focus first on the ENP profiles from the southern tip of Baja (stations 7–16), where conditions are appropriate for water column denitrification. As described above, the relationship between the NO_3^- N and O isotopes within the

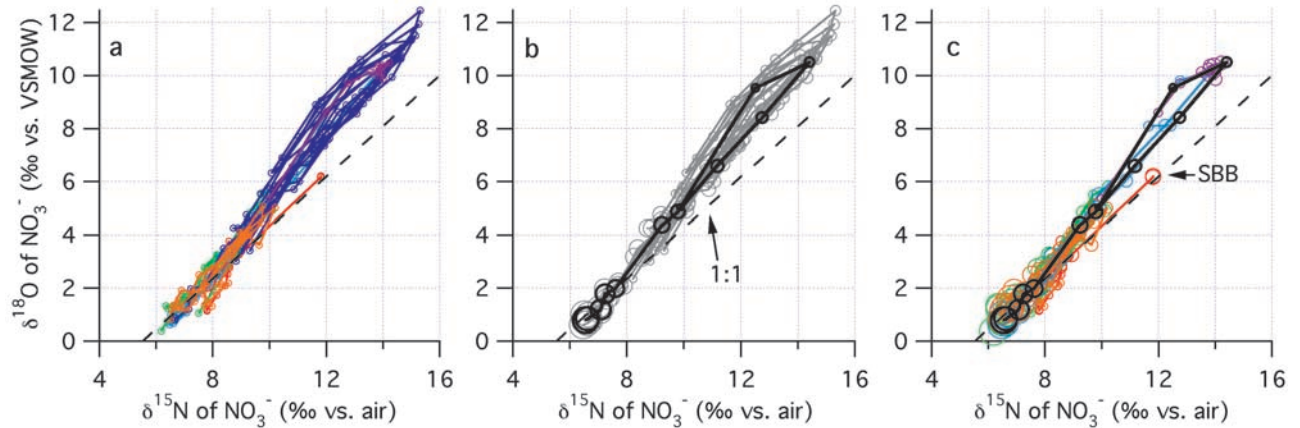


Figure 4. $\text{NO}_3^- \delta^{18}\text{O}$ versus $\text{NO}_3^- \delta^{15}\text{N}$ (a) for all data reported here, (b) for OXMZ01MV stations 7–16 (gray circles) and a depth-binned average profile (bold black circles), and (c) for the station 7–16 average (bold black circles) and the individual OXMZ01MV stations (2–8, 17–20) farther north of the tip of Baja along the California margin. In Figures 4b and 4c, the symbol size is proportional to sample water depth, scaled to a maximum water depth of 1450 m.

suboxic zone (200–800 m) cannot be explained solely by denitrification with an $^{18}\epsilon:^{15}\epsilon \sim 1$, especially in its shallow portion (e.g., at ~ 200 m). Graphically, the discrepancy from a 1:1 fractionation relationship expected for denitrification can be visualized as the horizontal distance in $\delta^{18}\text{O}$ -versus- $\delta^{15}\text{N}$ space between the data and a line with a slope ($^{18}\epsilon/^{15}\epsilon$) of 1 appropriate for denitrification running through the mean $\delta^{15}\text{N}$ and $\delta^{18}\text{O}$ of ENP deep water (Figure 4a). We formalize this as “ $\Delta(15,18)$ ”,

$$\Delta(15,18) \equiv (\delta^{15}\text{N} - \delta^{15}\text{N}_m) - \left(^{15}\epsilon/^{18}\epsilon \right) \times (\delta^{18}\text{O} - \delta^{18}\text{O}_m), \quad (1)$$

where $\delta^{15}\text{N}_m$ and $\delta^{18}\text{O}_m$ are the mean $\delta^{15}\text{N}$ and $\delta^{18}\text{O}$ of eastern North Pacific deep water, which is taken to approximate the source of NO_3^- to the upper water column of the eastern North Pacific, and $^{18}\epsilon:^{15}\epsilon$ is the N-to-O isotope effect ratio for denitrification, which our culture studies indicate to be 1 [Granger *et al.*, 2004a]. We use here 5‰ and -0.5 ‰ for $\delta^{15}\text{N}_m$ and $\delta^{18}\text{O}_m$ (based on samples taken from 3500 m and below at HOT station ALOHA (D. M. Sigman and D. Karl, unpublished data, 2005)), such that the 800–1450 m data from stations 7–16 yield a $\Delta(15,18)$ close to 0‰ (+0.2‰, Table 1) (see endnote v in Auxmat1.txt).

[25] For stations 7–16, $\Delta(15,18)$ varies coherently with depth (Figure 5c), being close to zero below 800 m (by definition) and decreasing upward to a minimum of -2.5 ‰ at 200 m, with a sharp increase to 100 m and above. The minimum in $\Delta(15,18)$ is ≥ 100 m shallower than the $\delta^{15}\text{N}$ maximum (Figure 5b) and the N^* minimum (Figure 5e). Given that the deviation is not proportional to $\delta^{15}\text{N}$ or N^* , it is not well explained by a uniform deviation in $^{18}\epsilon:^{15}\epsilon$ from the culture-derived estimate of 1. Moreover, this sense of deviation would require an $^{18}\epsilon:^{15}\epsilon > 1$, for which there is no support from previous work in seawater or freshwater. Finally, an $^{18}\epsilon:^{15}\epsilon$ of 1 yields an excellent fit to the data

from the Santa Barbara Basin (indicated red circles in Figure 4c), in which denitrification is progressively drawing down NO_3^- after a springtime flushing event [Sigman *et al.*, 2003b].

4.2. Regional Extent of the $\Delta(15,18)$ Minimum

[26] The ~ 200 -m-centered minimum in $\Delta(15,18)$ weakens as one moves north along the California margin and is not evident near Point Conception (Figure 6). The shallowest samples in the more northern profiles tend to reach positive values for $\Delta(15,18)$, which can be explained as a result of the algal uptake/remineralization cycle (see below). The lack of a strong $\Delta(15,18)$ minimum in the more northern profiles rules out the possibility that the minimum near the tip of Baja originates from advection from the north, for instance, because of a negative $\Delta(15,18)$ in preformed NO_3^- from regions of ventilation to the north. Comparison with Hawaii Ocean Time series station ALOHA shows clearly that the $\Delta(15,18)$ minimum in the ENP is also not transported into the eastern North Pacific margin from the west (D. M. Sigman and D. Karl, unpublished data, 2005). While it is still possible that the suboxic zone to the South represents a source for the $\Delta(15,18)$ minimum in the ENP near the tip of Baja, the data in hand indicate no role for transport and suggest that the $\Delta(15,18)$ minimum is generated locally.

[27] One aspect of the $\Delta(15,18)$ minimum that seems to have a simple cause is the upward increase in $\Delta(15,18)$ from

Table 1. Water Column Parameters for Model Targets

Parameters	Stations 7–16, 200–800 m	Stations 7–16, 800–1450 m	Difference, Shallow-Deep
$[\text{NO}_3^-]$, μM	33.79	44.29	-10.50
N^* , μM	-12.59	-6.35	-6.24
$\delta^{15}\text{N}$, ‰ versus air	11.39	7.02	4.37
$\delta^{18}\text{O}$, ‰ versus VSMOW	7.04	1.32	5.72
$\Delta(15,18)$, ‰	-1.15	0.20	-1.35

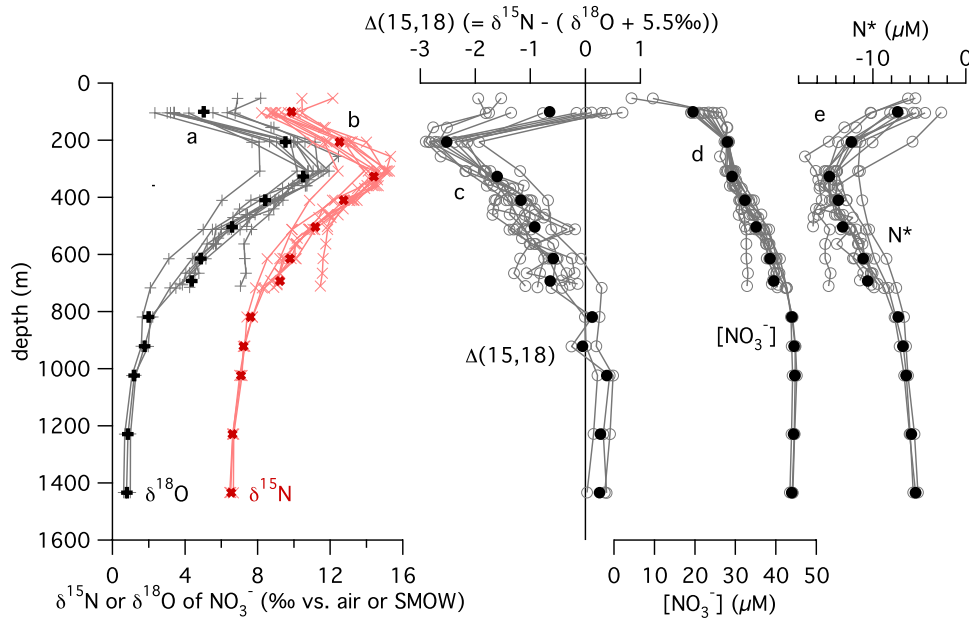


Figure 5. For OXMZ01MV stations 7–16, depth profiles of (a) NO_3^- $\delta^{18}\text{O}$ (gray pluses), (b) NO_3^- $\delta^{15}\text{N}$ (red crosses), (c) $\Delta(15,18)$, (d) $[\text{NO}_3^-]$, and (e) N^* . Also shown are depth-binned averages of these parameters for stations 7–16 (bold symbols).

the 200 m minimum toward the surface; this is well explained by the NO_3^- assimilation/remineralization cycle. The lack of significant surface NO_3^- in the region indicates that upwelled NO_3^- is consumed to completion by algal uptake. Thus the organic matter produced and exported into the subsurface will have the same $\delta^{15}\text{N}$ as the upwelled NO_3^- . However, the nitrification of this organic N produces NO_3^- with a $\delta^{18}\text{O}$ of $\sim 0\text{‰}$ (i.e., close to that of water), essentially “washing” the ^{18}O enrichment from the NO_3^- pool. This should tend to increase the $\Delta(15,18)$ as one approaches the top of the thermocline. Indeed, $\Delta(15,18)$ reaches positive values in many cases (Figures 5 and 6), most likely because of this effect. These samples are evident

in $\delta^{18}\text{O}$ -vs- $\delta^{15}\text{N}$ space as the points that reach below the 1:1 line in the lower left sector of the plot (Figures 4a and 4c).

4.3. Cause of the $\Delta(15,18)$ Minimum

[28] Owing to space limitations, we restrict ourselves to describing our two candidate explanations for the observed $\Delta(15,18)$ minimum, relegating a more complete discussion of other relevant processes to the Auxiliary Materials (see endnote vi in Auxmat1.txt [Altabet et al., 1991; Altabet and Francois, 2001; Bender, 1990; Böhlke et al., 2003; Casciotti et al., 2002, 2003; Fritz et al., 1989; Fry et al., 1991; Granger et al., 2004a, 2004b; Lehmann et al., 2004; Libes and Deuser, 1988; Lourey et al., 2003; Mariotti et al.,

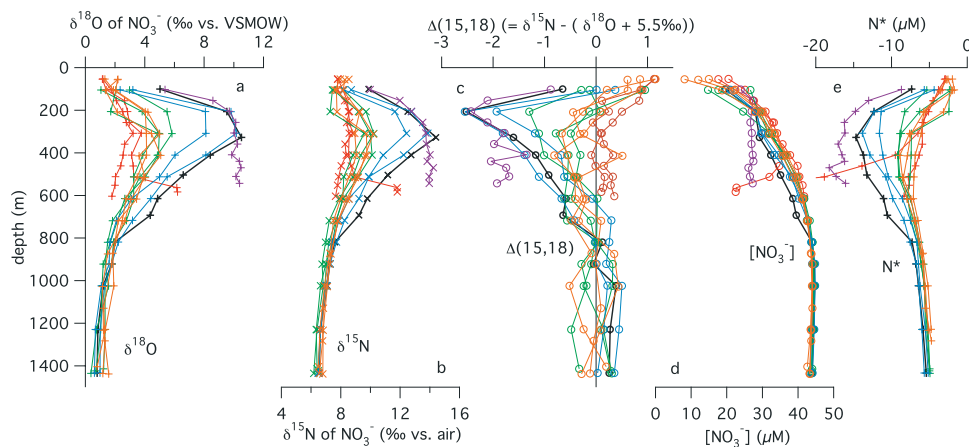


Figure 6. Comparison of the depth-binned average profile from OXMZ01MV stations 7–16 (bold black symbols) with individual OXMZ01MV stations 2–8 and 17–20 from farther north along the California margin (colors follow Figure 2). Depth profiles of (a) NO_3^- $\delta^{18}\text{O}$, (b) NO_3^- $\delta^{15}\text{N}$, (c) $\Delta(15,18)$, (d) $[\text{NO}_3^-]$, and (e) N^* .

1981; *Ostrom et al.*, 2000; *Thunell et al.*, 2004; *van Geen et al.*, 2003; *Voss et al.*, 1997; *Wada et al.*, 1987; *Waser et al.*, 1998]).

4.3.1. N₂ Fixation

[29] In the subtropical thermocline of the North Atlantic and North Pacific, there is evidence for the production of a sizable NO₃⁻ excess relative to expectations based on PO₄³⁻ concentration and Redfield ratios; this finding has been interpreted to indicate that newly fixed N is accumulating as NO₃⁻ in the thermocline waters of these regions [*Deutsch et al.*, 2001; *Gruber and Sarmiento*, 1997; *Hansell et al.*, 2004; *Michaels et al.*, 1996]. NO₃⁻ in the subtropical thermocline of both the Pacific and the North Atlantic has been observed to have a low δ¹⁵N, as low as 2‰ [*Karl et al.*, 2002; *Knapp et al.*, 2005; *Liu et al.*, 1996]. Given the low δ¹⁵N of newly fixed N, the low δ¹⁵N of subtropical thermocline NO₃⁻ is consistent with the N*-based interpretation of the accumulation of newly fixed N as thermocline NO₃⁻ [*Gruber and Sarmiento*, 1997]. More work is needed to validate this interpretation, but it would seem difficult for it to be strictly incorrect.

[30] On the basis of similar logic, *Brandes et al.* [1998] explain the upward decrease in δ¹⁵N above denitrification zones in the Arabian Sea and eastern tropical North Pacific as the result of oxidation of low-δ¹⁵N, newly fixed N to NO₃⁻. This explanation fits with the upward change in the δ¹⁸O/δ¹⁵N relationship reported here. That is, the shallower δ¹⁸O maximum suggests that the nitrification of newly fixed N is “eroding” the tops of the NO₃⁻ δ¹⁵N maximum and the N* minimum. It is not clear whether nitrification would be limited within the suboxic zone of our study region [*Lipschultz et al.*, 1990]. In any case, the suboxia does not extend far offshore at the latitudes of our stations [*Conkright et al.*, 2002], so NO₃⁻ could be produced from nitrification in the oxic waters just to the west and imported along isopycnals.

[31] As described above, the upward increase in Δ(15,18) above its minimum at 200 m is well explained by complete assimilation of upwelled NO₃⁻ and subsequent remineralization of most of the exported organic N in the shallow subsurface. That the minimum in Δ(15,18) is strongest at 200 m and not deeper could be explained by (1) the lower [NO₃⁻] at shallower depths, which requires a smaller amount of newly fixed N to cause the same decrease in Δ(15,18), (2) the tendency for nitrification at the upper margin of the suboxic zone [*Lipschultz et al.*, 1990], and/or (3) the rapid decrease in the sinking N flux with depth in the water column.

4.3.2. Nitrate/Nitrite Redox Cycling

[32] Since the work of *Anderson* [*Anderson*, 1982; *Anderson et al.*, 1982], it has been hypothesized that there is significant redox cycling between nitrate and nitrite in ocean suboxic zones, with NO₃⁻ reduction to NO₂⁻ in the core of the suboxic zones, mixing of the NO₂⁻ to the margins of the suboxic zone, and reoxidation of the NO₂⁻ once it reaches higher [O₂] waters. *Anderson* suggested that roughly half of the nitrate reduction in open ocean suboxic zones can be coupled to nitrite oxidation, the other half proceeding to denitrification. This exact process is not plausibly significant in our study region, as the measured [NO₂⁻] rarely climbed

above 0.05 μM (typically ~0.01 μM) in the subsurface samples. However, there might be exchange along isopycnals with waters to the south where that process could occur. Moreover, there might well be simultaneous NO₃⁻ reduction and NO₂⁻ oxidation in the same water parcel within our study region [*Lipschultz et al.*, 1990].

[33] Such a cycle might explain the deviation of NO₃⁻ δ¹⁸O and δ¹⁵N from 1:1 covariation. NO₃⁻ reduction will consume NO₃⁻ with the N and O isotope effects of denitrification. If the ambient NO₃⁻ δ¹⁵N and δ¹⁸O are 14‰ and 10‰, respectively, an isotope effect of 20‰ (for both N and O) will make the consumed NO₃⁻ approximately -6‰ and -10‰, respectively. When the NO₂⁻ produced is reoxidized to NO₃⁻, it will return NO₃⁻ with roughly the same δ¹⁵N as the loss, so that the ambient NO₃⁻ δ¹⁵N is, in net, unchanged. The δ¹⁸O of the reoxidized NO₃⁻, however, would most likely be higher than the δ¹⁸O of the NO₃⁻ consumed. The preferential extraction of ¹⁶O from the chain of N species (i.e., a “branching fractionation”) yields NO₂⁻ with a δ¹⁸O higher than that of the NO₃⁻ consumed [*Casciotti et al.*, 2002], such that its recycling back into the NO₃⁻ pool may cause a net increase in NO₃⁻ δ¹⁸O. In addition, the reduction to NO₂⁻ and reoxidation to NO₃⁻ will work to incorporate O atoms from H₂O, such that the reoxidized NO₃⁻ would likely be shifted toward a δ¹⁸O of 0‰. This shift might be complete if there is rapid O atom exchange with water in the enzyme active site of NO₂⁻ oxidase [*Dispirito and Hooper*, 1986], as has been observed to occur in the presence of enzymes catalyzing ammonium oxidation to NO₂⁻ [*Andersson et al.*, 1982]. Alternatively, the only O atoms added from H₂O may be the single O required to convert NO₂⁻ to NO₃⁻, so that the δ¹⁸O of NO₃⁻ from NO₂⁻ reoxidation has some memory of the δ¹⁸O of NO₂⁻ produced (as well as of NO₂⁻ reduction, which would increase the δ¹⁵N and δ¹⁸O of NO₂⁻; see below and endnote vii in *Auxmat1.txt* [*Bryan et al.*, 1983; *Casciotti*, 2002]). Details aside, the coupling of NO₃⁻ reduction and NO₂⁻ reoxidation should work to raise the δ¹⁸O of ambient NO₃⁻ relative to its δ¹⁵N, thereby generating a negative Δ(15,18).

[34] The plausibility of a role for the NO₃⁻/NO₂⁻ redox cycle in explaining the Δ(15,18) minimum is unclear. The minimum in Δ(15,18) at the top of the suboxic zone agrees with the expectation that the NO₃⁻/NO₂⁻ redox cycle would be most intense where the vertical [O₂] gradient is steepest [*Lipschultz et al.*, 1990]. It is troubling that NO₂⁻ is so scarce in this region of the ENP, although this does not absolutely preclude a tight balance between the reduction, release, and reoxidation of NO₂⁻. An additional argument against the NO₃⁻/NO₂⁻ redox cycle explanation for the Δ(15,18) minimum is the lack of any anomaly in Δ(15,18) associated with denitrification in the Santa Barbara Basin (Figure 4c), where we presume such a NO₃⁻/NO₂⁻ redox cycle should be equally active.

4.4. Steady State Model of the Candidate Processes

[35] We describe the results from the simplest possible quantitative model that we could conceive to estimate the fluxes of the two alternative processes that we have proposed to explain the Δ(15,18) minimum (Figure 7). This model represents the effects of five N cycle processes acting

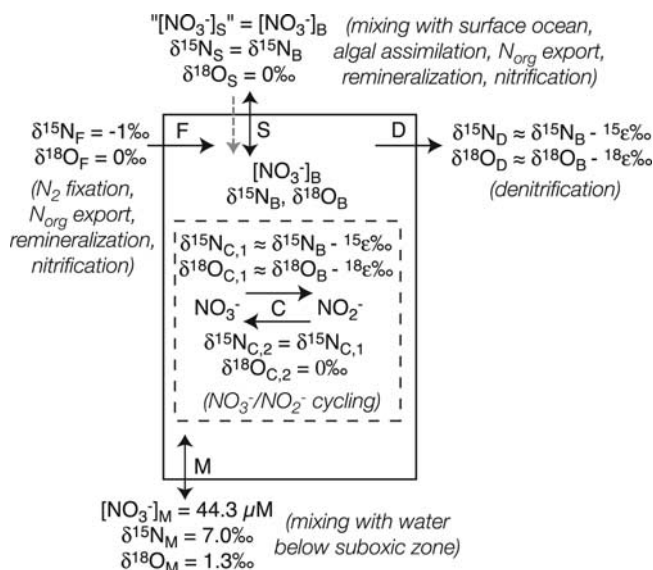


Figure 7. Steady state model of a water parcel (B for box) in the suboxic thermocline of the ENP. Five processes are included: (1) mixing with the deeper ENP (M; conditions taken from 800–1450 m data; see Table 1) (2) denitrification (D), (3) addition of NO_3^- from newly fixed N (F, one plausible explanation for the $\Delta(15,18)$ minimum; see text and Figure 8), (4) an internal cycle of NO_3^- reduction and NO_2^- oxidation (C, a second plausible explanation for the $\Delta(15,18)$ minimum; see text and Figure 9), and (5) mixing with a biologically active and NO_3^- -deplete surface ocean (S; any NO_3^- mixed up to the surface is returned with the same $\delta^{15}\text{N}$ but a $\delta^{18}\text{O}$ of 0‰; dashed downward arrow indicates the sinking and remineralization of organic N). In the experiments below, the isotope effect amplitude for denitrification is chosen to simultaneously fit observations for NO_3^- deficit, NO_3^- $\delta^{15}\text{N}$ and NO_3^- $\delta^{18}\text{O}$. For runs with non-zero F (Figure 8), $^{15}\epsilon = ^{18}\epsilon = 18.9\%$. For runs with non-zero C (Figure 9), $^{15}\epsilon = ^{18}\epsilon = 30.7\%$.

simultaneously on the suboxic thermocline zone of the ENP: (1) mixing with the deeper ENP (M), (2) denitrification (D), (3) mixing with a biologically active and NO_3^- deplete surface ocean (S), (4) addition of NO_3^- from the nitrification of N from new N_2 fixation (F), and (5) redox cycling between NO_3^- and NO_2^- (C; C1 is NO_3^- reduction, C2 is NO_2^- oxidation). The following rules apply to the fluxes.

[36] 1. Mixing with deeper eastern North Pacific water (M in Figure 7) introduces NO_3^- with a concentration, $\delta^{15}\text{N}$, and $\delta^{18}\text{O}$ measured in the water below the suboxic zone by our study (Table 1), while it removes NO_3^- with whatever concentration and isotope composition occurs in the thermocline box.

[37] 2. Denitrification (D in Figure 7) consumes NO_3^- with a kinetic isotope effect that is equivalent for $^{15}\text{N}/^{14}\text{N}$ and $^{18}\text{O}/^{16}\text{O}$. The amplitude of the isotope effect is adjusted to fit the data and is reported below.

[38] 3. Mixing with the surface ocean (S in Figure 7) has no effect on $[\text{NO}_3^-]$ or NO_3^- $\delta^{15}\text{N}$ because all NO_3^- mixed

upward into the surface is consumed in the surface and exported as organic N back into the reservoir, where it is completely remineralized to NO_3^- . However, the nitrification of this organic N export produces NO_3^- with a $\delta^{18}\text{O}$ of 0‰, essentially ‘washing’ the ^{18}O enrichment from the NO_3^- .

[39] 4. The NO_3^- added from newly fixed N (F in Figure 7) has a $\delta^{15}\text{N}$ of -1% and a $\delta^{18}\text{O}$ of 0‰.

[40] 5. In the $\text{NO}_3^-/\text{NO}_2^-$ redox cycle (C in Figure 7), NO_3^- reduction (C1) occurs with the same $^{15}\epsilon$ and $^{18}\epsilon$ as denitrification (D). For a given $^{15}\epsilon$ for denitrification, the $\delta^{15}\text{N}$ of the NO_3^- reoxidized from NO_2^- depends on the relative amplitudes of $^{15}\epsilon$ for NO_2^- reduction and NO_2^- oxidation; we assume that these isotope effects are equal in the calculations but consider other cases in the text. The $\delta^{18}\text{O}$ of the NO_3^- reoxidized from NO_2^- depends on the same factors as does its $\delta^{15}\text{N}$; however, the $\delta^{18}\text{O}$ is also affected by two additional factors. First, ^{16}O is preferentially lost from the nitrogen species in the denitrification pathway [Casciotti *et al.*, 2002]. This “branching fractionation” during NO_3^- reduction (assumed here to be equivalent to the $^{18}\epsilon$ of nitrate consumption by denitrification) yields NO_2^- with a $\delta^{18}\text{O} \sim 18\%$ higher than that of the NO_3^- consumed, such that its recycling back into the NO_3^- pool may cause a net NO_3^- $\delta^{18}\text{O}$ increase. Second, incorporation of O from H_2O during (1) $\text{NO}_2^-/\text{H}_2\text{O}$ exchange and (2) NO_2^- oxidation drives the $\delta^{18}\text{O}$ of the reoxidized NO_3^- toward 0‰. While Figure 7 shows only the case for complete O exchange between NO_2^- and H_2O , the cases of complete O exchange and no exchange are both considered in the calculations below. For lack of better information, we assume that the $^{18}\epsilon/^{15}\epsilon$ ratio is the same for NO_2^- reduction as for NO_2^- oxidation, regardless of what that ratio might be.

[41] Here we consider only the model steady state. Varying D, F, and C, we fit $[\text{NO}_3^-]$, NO_3^- $\delta^{15}\text{N}$, and $\Delta(15,18)$ for the means for the 200–800 m depth zone from stations 7–16, using the 800–1450 m data from the same stations to estimate the values for background ENP conditions (Table 1). The nitrate isotopes and N^* of the 800–1450 m water indicate that it is impacted by denitrification, by exchange with the eastern tropical Pacific suboxic zones and by sedimentary denitrification (P. DiFiore, unpublished results, 2005), and is thus far from reflecting the mean conditions of the global ocean or even the whole North Pacific. We address here only the fluxes that drive the isotopic and concentration differences between the suboxic thermocline box and the 800–1450 m water below it.

[42] We opted here to use mixing with the deeper water from the same stations, as opposed to lateral exchange, as the mechanism for refreshing the 200–800 m suboxic thermocline box. This allowed the current study to be self-contained with respect to measurements. Efforts to use other mixing end-members (e.g., the thermocline from the open subtropical Pacific as measured at station ALOHA (D. M. Sigman and D. Karl, unpublished data, 2005) or the thermocline from our more northern stations (Figures 3 and 6)), yielded similar results that nevertheless require the consideration of additional factors (calculations not shown).

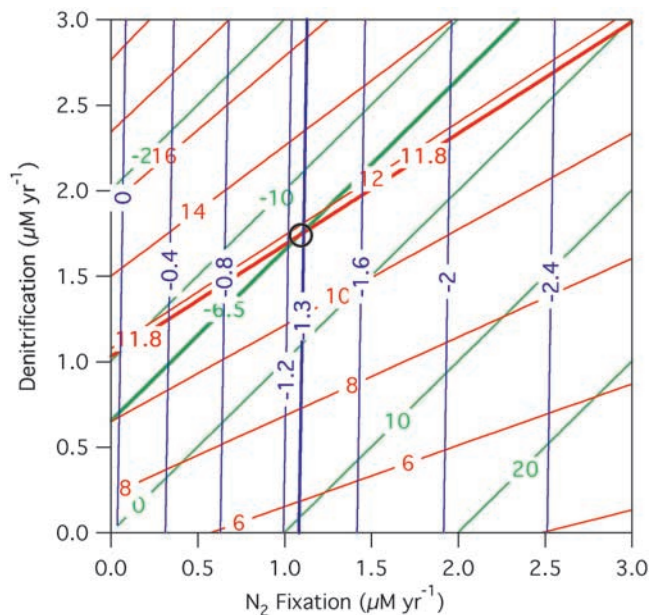


Figure 8. Application of the steady state model shown in Figure 7 to estimate the relative magnitude of the putative N_2 fixation input F relative to the denitrification loss D . Overlain are contour plots of $[NO_3^-]_B - [NO_3^-]_M$ (a measure of the NO_3^- deficit in the model box relative the deeper ENP, green), $\delta^{15}N_B$ (the $\delta^{15}N$ of NO_3^- in the thermocline box, red), and $\Delta(15,18)$ (blue) as a function of F and D . Thick lines indicate the appropriately weighted mean values of these parameters for the depth range 200–800 m in stations 7–16, and the black circle denotes their convergence where the model fits all three parameters simultaneously, yielding an estimate for the ratio of F to D of 0.65. See Table 1 for the data constraints used.

[43] The lack of a time-keeping constraint in our model means that we can only explore ratios of fluxes (i.e., the ratio of F or C to D), not the absolute magnitude of each flux. For flux magnitudes to be at least physically reasonable, we assume a value for M that yields a water residence time in the suboxic thermocline box of 10 years, intended to be roughly consistent with previous studies [Deutsch et al., 2001].

[44] Since F and C are alternative plausible explanations for the $\Delta(15,18)$ minimum, we explore these two terms separately in the sections below. However, they may both be at work.

4.4.1. Quantifying the Needed N_2 Fixation

[45] The results from the model are largely intuitive. First, more of an assumption than an observation, the difference in $[NO_3^-]$ between the suboxic thermocline box and the deeper water ($[NO_3^-]_B - [NO_3^-]_M$) is logically equivalent to the N^* difference from the deeper water, to which we refer below as the “ NO_3^- deficit” of the box. Second, the steady state NO_3^- deficit is affected solely by (and is proportional to) the ratio $(D - F)/M$. Since M is held constant in our calculations, Figure 8 indicates that the NO_3^- deficit is a function of $D - F$ (Figure 8, green contours). Third, $NO_3^- \delta^{15}N$ (and $\delta^{18}O$) increases with D and decreases with F (Figure 8, red contours). Fourth,

$\Delta(15,18)$ decreases as N_2 fixation increases, almost regardless of D (Figure 8, blue contours). Further visualization of model results are in the Auxiliary Materials (see endnote viii in Auxmat1.txt).

[46] In order to fit the 200–800 m data from stations 7–16 (Table 1), we find that the needed N_2 fixation/denitrification ratio (F/D) is roughly 0.65 (black circle in Figure 8). This suggests that 65% of the denitrification occurring in the 200–800 m suboxic zone is countered by the nitrification of newly fixed N . N^* in the suboxic zone (200–800 m) is $6.2 \mu M$ lower than in the deeper waters between 800 and 1450 m ($-12.6 \mu M$ and $-6.4 \mu M$, respectively; Table 1). Thus our results would require that N_2 fixation is erasing a NO_3^- deficit of $(0.65/(1 - 0.65)) \times 6.2 \mu M$, or $-11.6 \mu M$. Added to the observed N^* of $-12.6 \mu M$, this would yield a N^* in the suboxic zone of $-24.2 \mu M$, were it not for N_2 fixation, that is, a total N^* minimum of roughly twice the observed amplitude.

[47] The isotope effect for denitrification that is required to simultaneously fit the N^* , $NO_3^- \delta^{15}N$, and $NO_3^- \delta^{18}O$ (or $\Delta(15,18)$) data is 18.9‰, ~ 5 –10‰ lower than derived previously from regression of $NO_3^- \delta^{15}N$ against N^* in field data [Altabet et al., 1999; Brandes et al., 1998; Sigman et al., 2003b]. The need for a lower isotope effect than previous field studies at least partially arises from our isotope-derived inference that N_2 fixation causes the N^* -derived NO_3^- deficit to be less than the actual amount of NO_3^- consumed by denitrification. While the true biological isotope effect amplitude for denitrifiers in the ENP is not known, the value required by the model may be lower than that value, in which case it may indicate that a fraction of the NO_3^- consumption occurring within the suboxic zone is driven by sedimentary denitrification along the margin [Sigman et al., 2003b]. However, the isotope effect amplitude required by the model would also increase modestly if spatial heterogeneity were included in the model [Deutsch et al., 2004].

[48] The assimilation/remineralization cycle (S in Figure 7), in the case of complete NO_3^- consumption in the surface, decreases $NO_3^- \delta^{18}O$ toward its nitrification production value (~ 0 ‰) while not affecting $NO_3^- \delta^{15}N$; in net, the effect is to increase $\Delta(15,18)$, that is, erode the $\Delta(15,18)$ minimum (see above). We neglect this term in the calculation shown in Figure 8, setting S to 0. Including this term would yield an even higher N_2 fixation/denitrification ratio (see endnote ix in Auxmat1.txt), but estimating the amplitude of S is difficult.

4.4.2. Quantifying the Needed Nitrate/Nitrite Redox Cycling

[49] Because there is essentially no NO_2^- in this region of the ENP, if the signal is generated locally, a putative NO_3^-/NO_2^- redox cycle must occur within a given water sample (i.e., without NO_2^- transport). Thus we can meaningfully compare the model results to the peak amplitude of the $\Delta(15,18)$ minimum (-2.51 ‰) at 200 m as well as to the mean $\Delta(15,18)$ of the 200–800 m interval (-1.15 ‰, Figure 9, dotted and solid gray bars, respectively). For the cases considered here, NO_2^- oxidation must be ~ 0.7 – 0.95 and ~ 0.35 – 0.45 times the rate of NO_2^- reduction to fit the observations at 200 m and over the 200–800 m

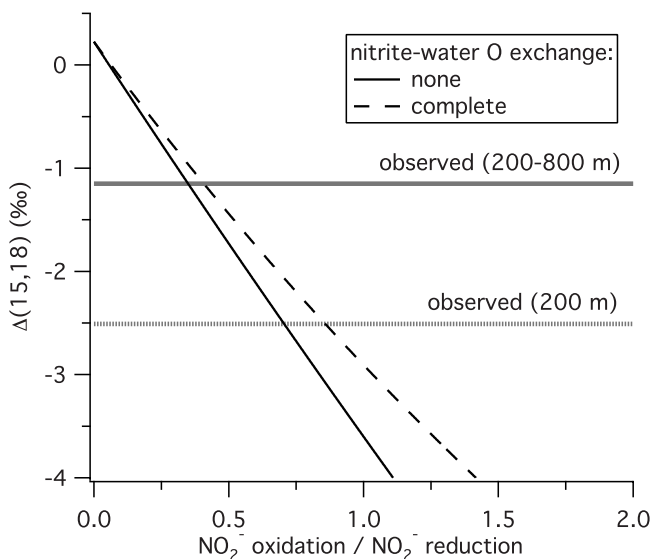


Figure 9. For the same model, $\Delta(15,18)$ plotted versus C/D (the NO_2^- oxidation/ NO_2^- reduction ratio) for the scenario where the $\Delta(15,18)$ minimum is caused by a $\text{NO}_3^-/\text{NO}_2^-$ redox cycle. The model results are compared to the peak amplitude of the $\Delta(15,18)$ minimum (-2.51‰) at 200 m and to the mean $\Delta(15,18)$ of the 200–800 m interval (-1.15‰ ; dotted and solid gray bars, respectively). In these simulations, D was set to match the target $[\text{NO}_3^-]_{\text{B}} - [\text{NO}_3^-]_{\text{M}}$ (Table 1) and $\delta^{15}\text{N}_{\text{B}}$ was matched by adjusting the denitrification $^{15}\epsilon = ^{18}\epsilon$ to 30.7‰. The $\delta^{18}\text{O}$ of NO_2^- produced is made $^{18}\epsilon\text{‰}$ higher than the NO_3^- reduced to take into account the preferential ^{16}O loss during NO_3^- reduction (see text). Then the reoxidized NO_3^- is nudged toward a $\delta^{18}\text{O}$ of 0‰, (1) by 33% in the case of one O atom added from water to form NO_3^- but no O atom exchange of NO_2^- with water (solid line) or (2) by 100% in the case of complete O atom exchange (dashed line). Lacking better information, we have assumed that (1) the $^{15}\epsilon$ for NO_2^- oxidation is the same as the $^{15}\epsilon$ for NO_2^- reduction and (2) that the $^{18}\epsilon/^{15}\epsilon$ ratio is the same for NO_2^- reduction as for NO_2^- oxidation (the value of that ratio having no effect in this case).

interval, respectively (Figure 9). The preference for $^{16}\text{O}-\text{NO}_3^-$ during NO_3^- reduction and the preferential extraction of ^{16}O from the NO_2^- produced (the “branching fractionation”), which we assume here to have the same $^{18}\epsilon$, offset one another to yield NO_2^- with a $\delta^{18}\text{O}$ close to that of the NO_3^- in the water and thus $<10\text{‰}$ greater than the $\delta^{18}\text{O}$ of the water. Therefore, for a given amount of $\text{NO}_3^-/\text{NO}_2^-$ cycling, the case of no $\text{NO}_2^-/\text{H}_2\text{O}$ exchange yields only slightly greater $\Delta(15,18)$ than the case with complete exchange (solid versus dashed line in Figure 9).

[50] The unknown isotope systematics of NO_2^- represent a major weakness in this modeling exercise (also see endnote x in Auxmat1.txt [Bryan *et al.*, 1983; Casciotti, 2002]). Nevertheless, the ratios given above for NO_2^- oxidation to reduction are generally within the range of those originally proposed as part of a transport cycle (0.65–1.50) [Anderson, 1982; Anderson *et al.*, 1982] or measured within individual

water samples [Lipschultz *et al.*, 1990]. However, we again note that those rates involved waters with 5–10 μM NO_2^- , whereas there is essentially no NO_2^- in our profiles. Thus, if the isotopic signal of this process is important, it may be through exchange with NO_2^- -bearing waters to the south.

5. Summary and Conclusions

[51] Here we report coupled N and O isotope measurements of NO_3^- from a set of hydrocast stations collected along the continental margin from Point Conception to the southern tip of Baja California. The isotope data from the California margin show a distinct anomaly in the $\delta^{18}\text{O}:\delta^{15}\text{N}$ relationship from expectations for denitrification alone, with $\delta^{15}\text{N}$ being lower than expected from $\delta^{18}\text{O}$. This isotope anomaly (described as a negative value for “ $\Delta(15,18)$ ”) is present from 200 to 800 m but peaks at 200 m, above the maximum in $\text{NO}_3^- \delta^{15}\text{N}$. Comparison of the data from the tip of Baja with the stations from further north and with data from near Hawaii (D. M. Sigman and D. Karl, unpublished data, 2005) indicates that the anomaly originates in or near the region of denitrification.

[52] One plausible explanation for the $\Delta(15,18)$ minimum is the addition of low- $\delta^{15}\text{N}$ NO_3^- to the shallow thermocline in the same region where denitrification occurs, which “erodes” the tops of the denitrification-driven maximum in $\text{NO}_3^- \delta^{15}\text{N}$ and minimum in N^* . The most likely origin of this low- $\delta^{15}\text{N}$ NO_3^- is N_2 fixation in the surface ocean, the rain of this newly fixed N out of the surface ocean, and the subsequent nitrification of its products to NO_3^- in the thermocline. This is consistent with a previous interpretation of $\text{NO}_3^- \delta^{15}\text{N}$ data alone from the eastern tropical North Pacific and Arabian Sea that N_2 fixation was adding significant amounts of low- $\delta^{15}\text{N}$ NO_3^- to the shallow thermocline in these regions [Brandes *et al.*, 1998]. We use the coupled N and O isotope data, in the context of a simple model, to estimate that the rate of this putative N_2 fixation is roughly 0.65 of the rate of water column denitrification in the same region.

[53] Were the N_2 fixation input found to be the correct explanation for the $\Delta(15,18)$ minimum, it would indicate that a significant fraction of the NO_3^- loss to denitrification is subsequently compensated by N_2 fixation in the surface waters overlying or adjacent to the zone of denitrification. This would explain why PO_4^{3-} -bearing waters are not observed penetrating far into the eastern ranges of the Pacific subtropical gyres: N_2 fixers strip out this P in the waters proximal to the upwelling zones. Moreover, it would bolster the view that oceanic N_2 fixation is strongly controlled by N/P variations in the waters supplied to the surface, with diazotrophs succeeding under N-poor, P-bearing conditions [Broecker and Peng, 1982; Redfield, 1958; Tyrrell, 1999], a situation that has been demonstrated in lakes [Schindler, 1977; Smith, 1983].

[54] An alternative plausible mechanism for the development of the $\Delta(15,18)$ minimum is the redox cycling of NO_3^- and NO_2^- within suboxic zones. The logic is that $\text{NO}_3^- \delta^{18}\text{O}$ can be gradually increased if the NO_3^- reduced to NO_2^- is lower in $\delta^{18}\text{O}$ than the NO_3^- produced from the reoxidation of NO_2^- . However, the isotope dynamics of NO_2^- are poorly understood and essentially unknown in the case of the O

isotopes. For reasonable assumptions, the mechanism can explain the $\Delta(15,18)$ minimum with a ratio of NO_2^- oxidation to NO_2^- reduction of as little as 0.7.

[55] Looking forward, several routes can be imagined that should allow for these two plausible explanations to be tested. First, work on the isotope systematics of NO_2^- (especially the O isotope systematics) is clearly needed and would provide an immediate test of the premises behind the $\text{NO}_3^-/\text{NO}_2^-$ redox cycling scenario. Second, studies of other ocean regions, including model systems such as well-described isolated basins, would provide critical constraints on the coupled N and O isotopic effects of both N_2 fixation and NO_3^- cycling through other oxidation states. For instance, it is not difficult to identify regions where N_2 fixation is occurring without denitrification, and vice versa.

[56] The isotopic impact of redox cycling of NO_3^- and NO_2^- represents something of a liability in the current study because of the uncertainties in its isotope systematics, especially with regard to the O isotopes. However, one can imagine circumstances where the rate of cyclic consumption and production of NO_3^- could be well constrained by the N and O isotopes. At the base of the euphotic zone, a cycle of NO_3^- assimilation and remineralization back to NO_3^- should cause $\text{NO}_3^- \delta^{18}\text{O}$ to rise above the 1:1 $\delta^{18}\text{O}:\delta^{15}\text{N}$ increase expected from NO_3^- assimilation alone, because the $\delta^{18}\text{O}$ of the NO_3^- being consumed by assimilation is lower than the $\delta^{18}\text{O}$ of NO_3^- being produced by remineralization/nitrification [Granger *et al.*, 2004b]. In this case, the N and O isotopes should allow for the NO_3^- recycling to be more accurately quantified.

[57] **Acknowledgments.** We thank M. Bender, K. Casciotti, C. Deutsch, N. Gruber, and B. Ward for discussions. This work was supported by U.S. NSF OCE-0136449 and Biocomplexity grants OCE-9981479 (to D. M. S., through the MANTRA project) and DEB-0083566 (to Simon Levin), and by British Petroleum and Ford Motor Company through the Carbon Mitigation Initiative at Princeton University. M. F. L. acknowledges support from the DFG through grant LE 1326/1-1. Cruise OXMZ01MV was supported by grant NSF OCE 9809026.

References

- Altabet, M. A., and R. François (2001), Nitrogen isotope biogeochemistry of the Antarctic polar frontal zone at 170 degrees W, *Deep Sea Res. Part II*, 48, 4247–4273.
- Altabet, M. A., W. G. Deuser, S. Honjo, and C. Stienen (1991), Seasonal and depth-related changes in the source of sinking particles in the North Atlantic, *Nature*, 354, 136–139.
- Altabet, M. A., C. Pilskaln, R. Thunell, C. Pride, D. Sigman, F. Chavez, and R. Francois (1999), The nitrogen isotope biogeochemistry of sinking particles from the margin of the eastern North Pacific, *Deep Sea Res. Part I*, 46, 655–679.
- Anbar, M., and S. Gutmann (1961), The catalytic effect of chloride ions on the isotopic oxygen exchange of nitric and bromic acids with water, *J. Am. Chem. Soc.*, 83, 4741–4745.
- Anderson, J. J. (1982), The nitrite oxygen interface at the top of the oxygen minimum zone in the eastern tropical North Pacific, *Deep Sea Res., Part A*, 29, 1193–1201.
- Anderson, J. J., A. Okubo, A. S. Robbins, and F. A. Richards (1982), A model for nitrite and nitrate distributions in oceanic oxygen minimum zones, *Deep Sea Res., Part A*, 29, 1113–1140.
- Andersson, K. K., S. B. Philson, and A. B. Hooper (1982), ^{18}O isotope shift in ^{15}N NMR analysis of biological N-oxidations: $\text{H}_2\text{O}-\text{NO}_2^-$ exchange in the ammonia-oxidizing bacterium *Nitrosomonas*, *Proc. Natl. Acad. Sci. U. S. A.*, 79, 5871–5875.
- Barford, C. C., J. P. Montoya, M. A. Altabet, and R. Mitchell (1999), Steady-state nitrogen isotope effects of N_2 and N_2O production in *Paracoccus denitrificans*, *Appl. Environ. Microbiol.*, 65, 989–994.
- Bender, M. L. (1990), The $\delta^{18}\text{O}$ of dissolved O_2 in seawater: A unique tracer of circulation and respiration in the deep-sea, *J. Geophys. Res.*, 95, 22,243–22,252.
- Böhlke, J. K., G. E. Erickson, and K. Revesz (1997), Stable isotope evidence for an atmospheric origin of desert nitrate deposits in northern Chile and southern California, *Chem. Geol.*, 136, 135–152.
- Böhlke, J. K., S. J. Mroczkowski, and T. B. Coplen (2003), Oxygen isotopes in nitrate: New reference materials for O-18:O-17:O-16 measurements and observations on nitrate-water equilibration, *Rapid Commun. Mass Spectrom.*, 17, 1835–1846.
- Botzcher, J., O. Strelbel, S. Voerkelius, and H. L. Schmidt (1990), Using isotope fractionation of nitrate nitrogen and nitrate oxygen for evaluation of microbial denitrification in a sandy aquifer, *J. Hydrol.*, 114, 413–424.
- Brandes, J. A., and A. H. Devol (1997), Isotopic fractionation of oxygen and nitrogen in coastal marine sediments, *Geochim. Cosmochim. Acta*, 61, 1793–1801.
- Brandes, J. A., and A. H. Devol (2002), A global marine fixed nitrogen isotopic budget: Implications for Holocene nitrogen cycling, *Global Biogeochem. Cycles*, 16(4), 1120, doi:10.1029/2001GB001856.
- Brandes, J. A., A. H. Devol, T. Yoshinari, D. A. Jayakumar, and S. W. A. Naqvi (1998), Isotopic composition of nitrate in the central Arabian Sea and eastern tropical North Pacific: A tracer for mixing and nitrogen cycles, *Limnol. Oceanogr.*, 43, 1680–1689.
- Broecker, W. S., and T.-H. Peng (1982), *Tracers in the Sea*, 690 pp., Lamont-Doherty Earth Obs., Palisades, N. Y.
- Bryan, B. A., G. Shearer, J. L. Skeeters, and D. H. Kohl (1983), Variable expression of the nitrogen isotope effect associated with denitrification of nitrite, *J. Biol. Chem.*, 258, 8613–8617.
- Bunton, C. A., E. A. Halevi, and D. R. Llewellyn (1952), Oxygen exchange between nitric acid and water: Part I, *J. Am. Chem. Soc.*, 74, 4913–4917.
- Carpenter, E., H. Harvey, B. Fry, and D. Capone (1997), Biogeochemical tracers of the marine cyanobacterium *Trichodesmium*, *Deep Sea Res., Part I*, 44, 27–38.
- Casciotti, K. L. (2002), Molecular and stable isotopic characterization of enzymes involved in nitrification and nitrifier-denitrification, Ph.D., Princeton Univ., Princeton, N. J.
- Casciotti, K. L., D. M. Sigman, M. G. Hastings, J. K. Böhlke, and A. Hilker (2002), Measurement of the oxygen isotopic composition of nitrate in seawater and freshwater using the denitrifier method, *Anal. Chem.*, 74, 4905–4912.
- Casciotti, K. L., D. M. Sigman, and B. B. Ward (2003), Linking diversity and stable isotope fractionation in ammonia-oxidizing bacteria, *Geomicrobiol. J.*, 20, 1–19, doi:10.1080/01490450390219887.
- Cline, J. D., and I. R. Kaplan (1975), Isotopic fractionation of dissolved nitrate during denitrification in the eastern tropical North Pacific Ocean, *Mar. Chem.*, 3, 271–299.
- Cline, J. D., and F. A. Richards (1972), Oxygen deficient conditions and nitrate reduction in the eastern tropical North Pacific Ocean, *Limnol. Oceanogr.*, 17, 885–900.
- Codispoti, L. A., *et al.* (1986), High nitrite levels off northern Peru—A signal of instability in the marine denitrification rate, *Science*, 233, 1200–1202.
- Codispoti, L. A., J. A. Brandes, J. P. Christensen, A. H. Devol, S. W. A. Naqvi, H. W. Paerl, and T. Yoshinari (2001), The oceanic fixed nitrogen and nitrous oxide budgets: Moving targets as we enter the anthropocene?, *Sci. Mar.*, 65, 85–101.
- Conkright, M. E., R. A. Locarnini, H. E. Garcia, T. D. O'Brien, T. P. Boyer, C. Stephens, and J. I. Antonov (2002), World Ocean Atlas 2001: Objective analyses, data statistics, and figures, CD-ROM documentation, report, 17 pp., Natl. Oceanogr. Data Cent., Silver Spring, Md.
- Delwiche, C. C., P. J. Zinke, C. M. Johnson, and R. A. Virginia (1979), Nitrogen isotope distribution as a presumptive indicator of nitrogen-fixation, *Bot. Gaz.*, 140, 65–69.
- Deutsch, C., N. Gruber, R. M. Key, J. L. Sarmiento, and A. Ganaschaud (2001), Denitrification and N_2 fixation in the Pacific Ocean, *Global Biogeochem. Cycles*, 15, 483–506.
- Deutsch, C., D. M. Sigman, R. C. Thunell, N. Meckler, and G. H. Haug (2004), Stable isotope constraints on the glacial/interglacial oceanic nitrogen budget, *Global Biogeochem. Cycles*, 18, GB4012, doi:10.1029/2003GB002189.
- Dispirito, A. A., and A. B. Hooper (1986), Oxygen-exchange between nitrate molecules during nitrite oxidation by nitrobacter, *J. Biol. Chem.*, 261, 10,534–10,537.
- Durka, W., E.-D. Schulze, G. Gebauer, and S. Voerkelius (1994), Effects of forest decline on uptake and leaching of deposited nitrate determined from ^{15}N and ^{18}O measurements, *Nature*, 372, 765–767.
- Fritz, P., G. M. Basharmal, R. J. Drimmie, J. Ibsen, and R. M. Qureshi (1989), Oxygen isotope exchange between sulphate and water during bacterial reduction of sulphate, *Chem. Geol.*, 79, 99–105.

- Fry, B., H. W. Jannasch, S. J. Molyneux, C. O. Wirsen, J. A. Muramoto, and S. King (1991), Stable isotope studies of the carbon, nitrogen and sulfur cycles in the Black Sea and the Cariaco Trench, *Deep Sea Res., Part A*, 38, S1003–S1019.
- Gonfiantini, R., W. Stichler, and K. Rosanski (1995), Standards and inter-comparison materials distributed by the IAEA for stable isotope measurements, report, Int. At. Energy Agency, Vienna.
- Granger, J., D. M. Sigman, M. F. Lehmann, and P. D. Tortell (2004a), Nitrogen and oxygen isotope effects associated with nitrate assimilation and denitrification by laboratory cultures of marine plankton, *Eos Trans. AGU*, 85(47), Fall Meet. Suppl., Abstract H51E-O52.
- Granger, J., D. M. Sigman, J. A. Needoba, and P. J. Harrison (2004b), Coupled nitrogen and oxygen isotope fractionation of nitrate during assimilation by cultures of marine phytoplankton, *Limnol. Oceanogr.*, 49, 1763–1773.
- Gruber, N., and J. L. Sarmiento (1997), Global patterns of marine nitrogen fixation and denitrification, *Global Biogeochem. Cycles*, 11, 235–266.
- Hansell, D. A., N. R. Bates, and D. B. Olson (2004), Excess nitrate and nitrogen fixation in the North Atlantic Ocean, *Mar. Chem.*, 84, 243–265.
- Hoering, T., and H. T. Ford (1960), The isotope effect in the fixation of nitrogen by *Azotobacter*, *J. Am. Chem. Soc.*, 82, 376–378.
- Karl, D., A. Michaels, B. Bergman, D. Capone, E. Carpenter, R. Letelier, F. Lipschultz, H. Paerl, D. Sigman, and L. Stal (2002), Dinitrogen fixation in the world's oceans, *Biogeochemistry*, 57/58, 47–98.
- Kendall, C. (1998), Tracing nitrogen sources and cycling in catchments, in *Isotope Tracers in Catchment Hydrology*, edited by C. Kendall and J. J. McDonnell, pp. 519–576, Elsevier, New York.
- Kienast, M. (2000), Unchanged nitrogen isotopic composition of organic matter in the South China Sea during the last climatic cycle: Global implications, *Paleoceanography*, 15, 244–253.
- Knapp, A. N., D. M. Sigman, and F. Lipschultz (2005), N isotopic composition of dissolved organic nitrogen and nitrate at the Bermuda Atlantic time-series study site, *Global Biogeochem. Cycles*, 19, GB1018, doi:10.1029/2004GB002320.
- Kumar, S., D. J. D. Nicholas, and E. H. Williams (1983), Definitive N-15 NMR evidence that water serves as a source of O during nitrite oxidation by *Nitrobacter-agilis*, *FEBS Lett.*, 152, 71–74.
- Lehmann, M. F., P. Reichert, S. M. Bernasconi, A. Barbieri, and J. A. McKenzie (2003), Modelling nitrogen and oxygen isotope fractionation during nitrate reduction in a hypolimnetic redox transition zone, *Geochim. Cosmochim. Acta*, 67, 2529–2542.
- Lehmann, M. F., D. M. Sigman, and W. M. Berelson (2004), Coupling the N-15/N-14 and O-18/O-16 of nitrate as a constraint on benthic nitrogen cycling, *Mar. Chem.*, 88, 1–20.
- Lehmann, M. F., D. M. Sigman, D. C. McCorkle, B. G. Brunelle, S. S. Hoffmann, M. Kienast, and J. Clement (2005), Origin of the deep Bering Sea nitrate deficit: Constraints from the nitrogen and oxygen isotopic composition of water column nitrate and benthic nitrate fluxes, *Global Biogeochem. Cycles*, 19, GB4005, doi:10.1029/2005GB002508.
- Libes, S. M., and W. G. Deuser (1988), The isotope geochemistry of particulate nitrogen in the Peru Upwelling Area and the Gulf of Maine, *Deep Sea Res., Part A*, 35, 517–533.
- Lipschultz, F., S. C. Wofsy, B. B. Ward, L. A. Codispoti, G. Friedrich, and J. W. Elkins (1990), Bacterial transformations of inorganic nitrogen in the oxygen-deficient waters of the eastern tropical South Pacific Ocean, *Deep Sea Res., Part A*, 37, 1513–1541.
- Liu, K.-K., and I. R. Kaplan (1989), The eastern tropical Pacific as a source of ¹⁵N-enriched nitrate in seawater off southern California, *Limnol. Oceanogr.*, 34, 820–830.
- Liu, K.-K., M. J. Su, C. R. Hsueh, and G. C. Gong (1996), The nitrogen isotopic composition of nitrate in the Kuroshio Water northeast of Taiwan: Evidence for nitrogen fixation as a source of isotopically light nitrate, *Mar. Chem.*, 54, 273–292.
- Lourey, M. J., T. W. Trull, and D. M. Sigman (2003), Sensitivity of $\delta^{15}\text{N}$ of nitrate, surface suspended and deep sinking particulate nitrogen to seasonal nitrate depletion in the Southern Ocean, *Global Biogeochem. Cycles*, 17(3), 1081, doi:10.1029/2002GB001973.
- Mariotti, A., J. C. Germon, P. Hubert, P. Kaiser, R. Letolle, A. Tardieux, and P. Tardieux (1981), Experimental determination of nitrogen kinetic isotope fractionation: Some principles; illustration for the denitrification and nitrification processes, *Plant Soil*, 62, 413–430.
- Mengis, M., S. L. Schiff, M. Harris, M. C. English, R. Aravena, R. J. Elgood, and A. MacLean (1999), Multiple geochemical and isotopic approaches for assessing ground water NO_3^- elimination in a riparian zone, *Ground Water*, 37, 448–457.
- Michaels, A. F., D. Olson, J. Sarmiento, J. Ammerman, K. Fanning, R. Jahnke, A. H. Knap, F. Lipschultz, and J. Prospero (1996), Transformations of nitrogen and phosphorus in the deep North Atlantic Ocean, *Biogeochemistry*, 35, 181–226.
- Middelburg, J. J., K. Soetaert, P. M. J. Herman, and C. H. R. Heip (1996), Denitrification in marine sediments: A model study, *Global Biogeochem. Cycles*, 10, 661–673.
- Needoba, J. A., D. M. Sigman, and P. J. Harrison (2004), The mechanism of isotope fractionation during algal nitrate assimilation as illuminated by the N-15/N-14 of intracellular nitrate, *J. Phycol.*, 40, 517–522.
- Ostrom, N. E., M. E. Russ, B. Popp, T. M. Rust, and D. M. Karl (2000), Mechanisms of nitrous oxide production in the subtropical North Pacific based on determinations of the isotopic abundances of nitrous oxide and di-oxygen, *Chemosphere—Global Change Sci.*, 2, 281–290.
- Pantoja, S., D. J. Repeta, J. P. Sachs, and D. M. Sigman (2002), Stable isotope constraints on the nitrogen cycle of the Mediterranean Sea water column, *Deep Sea Res., Part I*, 4, 1609–1621.
- Redfield, A. C. (1958), The biological control of chemical factors in the environment, *Am. Sci.*, 46, 205–221.
- Revesz, K., J. K. Böhlke, and Y. Yoshinari (1997), Determination of d^{18}O and d^{15}N in nitrate, *Anal. Chem.*, 69, 4375–4380.
- Schindler, D. W. (1977), Evolution of phosphorus limitation in lakes, *Science*, 195, 260–262.
- Sebilo, M., G. Billen, M. Grably, and A. Mariotti (2003), Isotopic composition of nitrate-nitrogen as a marker of riparian and benthic denitrification at the scale of the whole Seine River system, *Biogeochemistry*, 63, 35–51.
- Shearer, G., J. D. Schneider, and D. H. Kohl (1991), Separating the efflux and influx components of net nitrate uptake by *Synechococcus-R2* under steady-state conditions, *J. Gen. Microbiol.*, 137, 1179–1184.
- Sigman, D. M., and K. L. Casciotti (2001), Nitrogen isotopes in the ocean, in *Encyclopedia of Ocean Sciences*, edited by J. H. Steele, K. K. Turekian, and S. A. Thorpe, pp. 1884–1894, Elsevier, New York.
- Sigman, D. M., M. A. Altabet, D. C. McCorkle, R. Francois, and G. Fischer (2000), The d^{15}N of nitrate in the Southern Ocean: Nitrogen cycling and circulation in the ocean interior, *J. Geophys. Res.*, 105, 19,599.
- Sigman, D. M., K. L. Casciotti, M. Andreani, C. Barford, M. Galanter, and J. K. Böhlke (2001), A bacterial method for the nitrogen isotopic analysis of nitrate in seawater and freshwater, *Anal. Chem.*, 73, 4145–4153.
- Sigman, D. M., S. J. Lehman, and D. W. Oppo (2003a), Evaluating mechanisms of nutrient depletion and C-13 enrichment in the intermediate-depth Atlantic during the last ice age, *Paleoceanography*, 18(3), 1072, doi:10.1029/2002PA000818.
- Sigman, D. M., R. Robinson, A. N. Knapp, A. van Geen, D. C. McCorkle, J. A. Brandes, and R. C. Thunell (2003b), Distinguishing between water column and sedimentary denitrification in the Santa Barbara Basin using the stable isotopes of nitrate, *Geochem. Geophys. Geosyst.*, 4(5), 1040, doi:10.1029/2002GC000384.
- Silva, S. R., C. Kendall, D. H. Wilkison, A. C. Ziegler, C. C. Y. Chang, and R. J. Avanzino (2000), A new method for collection of nitrate from fresh water and the analysis of nitrogen and oxygen isotope ratios, *J. Hydrol.*, 228, 22–36.
- Smith, V. H. (1983), Low nitrogen to phosphorus ratios favor dominance by blue-green-algae in lake phytoplankton, *Science*, 221, 669–671.
- Thunell, R. C., D. M. Sigman, F. Muller-Karger, Y. Astor, and R. Varela (2004), The nitrogen isotope dynamics of the Cariaco Basin, Venezuela, *Global Biogeochem. Cycles*, 18, GB3001, doi:10.1029/2003GB002185.
- Tyrrell, T. (1999), The relative influences of nitrogen and phosphorus on oceanic primary production, *Nature*, 400, 525–531.
- van Geen, A. E. A. (2001), Baja California coring cruise OXMZ01MV: R/V *Melville*, October 29 – November 22, 1999, *Tech. Rep. LDEO 2001-01*, 300 pp., Lamont-Doherty Earth Obs., Palisades, N. Y.
- van Geen, A., Y. Zheng, J. M. Bernhard, K. G. Cannariato, J. Carriquiry, W. E. Dean, B. W. Eakins, J. D. Ortiz, and J. Pike (2003), On the preservation of laminated sediments along the western margin of North America, *Paleoceanography*, 18(4), 1098, doi:10.1029/2003PA000911.
- Voss, M., G. Nausch, and J. P. Montoya (1997), Nitrogen stable isotope dynamics in the central Baltic Sea: Influence of deep-water renewal on the N-cycle changes, *Mar. Ecol. Prog. Ser.*, 158, 11–21.
- Voss, M., J. W. Dippner, and J. P. Montoya (2001), Nitrogen isotope patterns in the oxygen-deficient waters of the eastern tropical North Pacific Ocean, *Deep Sea Res., Part I*, 48, 1905–1921.
- Wada, E., M. Terazaki, Y. Kabaya, and T. Nemoto (1987), N-15 and C-13 abundances in the Antarctic Ocean with emphasis on the biogeochemical structure of the food web, *Deep Sea Res., Part A*, 34, 829–841.
- Waser, N. A., K. D. Yin, Z. M. Yu, K. Tada, P. J. Harrison, D. H. Turpin, and S. E. Calvert (1998), Nitrogen isotope fractionation during nitrate, ammonium and urea uptake by marine diatoms and coccolithophores under various conditions of N availability, *Mar. Ecol. Prog. Ser.*, 169, 29–41.
- Wassenaar, L. I. (1995), Evaluation of the origin and fate of nitrate in the Abbotsford aquifer using the isotopes of N-15 and O-18 in NO_3^- , *Appl. Geochem.*, 10, 391–405.

Wooster, W. S., and J. H. Jones (1970), California Undercurrent off northern Baja California, *J. Mar. Res.*, 28, 235–250.

G. Cane, P. J. DiFiore, R. Ho, and D. M. Sigman, Department of Geosciences, Princeton University, Guyot Hall, Princeton, NJ 08544, USA. (sigman@princeton.edu)

J. Granger, Department of Earth and Ocean Sciences, University of British Columbia, 6270 University Blvd., Vancouver, British Columbia V6T 1Z4, Canada. (jgranger@eos.ubc.ca)

M. M. Lehmann, Geochemistry and Geodynamics Research Center (GEOTOP-UQAM-McGill), University of Quebec at Montreal, Montréal (Québec) H3C 3P8, Canada. (lehmann.moritz@uqam.ca)

A. van Geen, Lamont-Doherty Earth Observatory of Columbia University, Palisades, NY 10964, USA. (avangeen@ldeo.columbia.edu)